Seasonal and Local Solar Time Variation of the Meridional Wind at 95 km from Observations of the 11.072-GHz Ozone Line and the 557.7-nm Oxygen Line

ALAN E. E. ROGERS, PHILIP J. ERICKSON, AND LARISA P. GONCHARENKO

Haystack Observatory, Massachusetts Institute of Technology, Westford, Massachusetts

OMAR B. ALAM

School of Applied and Engineering Physics, Cornell University, Ithaca, New York

JOHN NOTO, ROBERT B. KERR,[a] AND SUDHA KAPALI

Scientific Solutions, Inc., North Chelmsford, Massachusetts

(Manuscript received 8 December 2015, in final form 31 March 2016)

ABSTRACT

Ground-based spectrometers have been deployed to measure the concentration, velocity, and temperature of ozone in the mesosphere and lower thermosphere (MLT), using low-cost satellite television electronics to observe the 11.072-GHz line of ozone. The ozone line was observed at an altitude near 95 km at 38°N, 71°W using three spectrometers located at the Massachusetts Institute of Technology's Haystack Observatory (Westford, Massachusetts), Chelmsford High School (Chelmsford, Massachusetts), and Union College (Schenectady, New York), each pointed south at 8° elevation. Observations from 2009 through 2014 were used to derive the nightly averaged seasonal variation of the 95-km altitude meridional wind velocity, as well as the seasonally averaged variation of the meridional wind with local solar time. The results indicate a seasonal trend in which the winds at 95 km are directed southward at about 10 m s^{-1} in the summer of the Northern Hemisphere and northward at about 10 m s^{-1} in the winter. Nighttime data from −5 to +5 local solar time show a gradual transition of the meridional wind velocity from about −20 to 20 m s^{-1}. These variations correlate well with nighttime wind measurements using 557.7-nm optical airglow observations from the Millstone Hill high-resolution Fábry–Perot interferometer (FPI) in Westford.

1. Introduction

The Mesospheric Ozone System for Atmospheric Investigations in the Classroom (MOSAIC) is an educational project focused on ground-based observations of the relatively weak microwave line of ozone at 11.072 454 5 GHz (Pickett et al. 1998) in the upper mesosphere using low-cost satellite television (TV) electronics. Along with its primary goal of providing locally acquired data to aid in the teaching of data analysis methods and statistics to high school students, MOSAIC provides an ongoing source of science-quality data on mesospheric ozone variations, and the data are publicly available online.[1] The ozone in the upper mesosphere is measured by MOSAIC using a satellite TV low-noise block downconverter, followed by an intermediate frequency downconverter and analog-to-digital converter. To increase the strength of the line, the antenna beam is pointed an elevation of 8° to increase the pathlength through the atmosphere. The ozone in the upper mesosphere is at low pressure, so a narrow Doppler broadened line originating from an altitude of about 95 km stands out

Denotes Open Access content.

[a] Current affiliation: Scientific Computing, Inc., Springfield, Virginia.

Corresponding author address: Alan E. E. Rogers, Haystack Observatory, Massachusetts Institute of Technology, Off Route 40, Westford, MA 01886-1299.
E-mail: arogers@haystack.mit.edu

[1] MOSAIC data are archived in the Madrigal distributed database system, supported by the U.S. National Science Foundation's Atmospheric and Geospace Sciences directorate for atmospheric studies (http://madrigal.haystack.mit.edu/).

DOI: 10.1175/JTECH-D-15-0247.1

from the pressure-broadened line from the ozone at lower altitudes. In this paper we assume a nominal altitude for the secondary maximum of the nighttime ozone to be 95 km (Smith and Marsh 2005). We also assume based on satellite measurements (Gao et al. 2012) that the 557.7-nm oxygen line originates from the same altitude. A complete description of the instrument and measurements of the seasonal and diurnal variations of ozone near the mesopause for data collected in 2008 were reported by Rogers et al. (2009). The repeatability of seasonal mesospheric ozone variations from 2008 through 2011 at six sites in the northeastern United States was reported by Rogers et al. (2012). While the observed line is only about 20 mK out of a background system noise of about 100 K, it is nevertheless possible to estimate the average velocity of the ozone from the small shift in the line center frequency due to the Doppler shift from the wind at 95 km. In this paper, we report the average nighttime mesospheric wind from three spectrometers located at the Massachusetts Institute of Technology (MIT)'s Haystack Observatory (Westford, Massachusetts), Chelmsford High School (Chelmsford, Massachusetts), and Union College (Schenectady, New York) using data from 2010 through 2014. These sites have their antenna beams pointing south, allowing the measurement of the meridional wind at a latitude of 38°N and a longitude around 71°W, where the antenna beams intersect the region at 95 km.

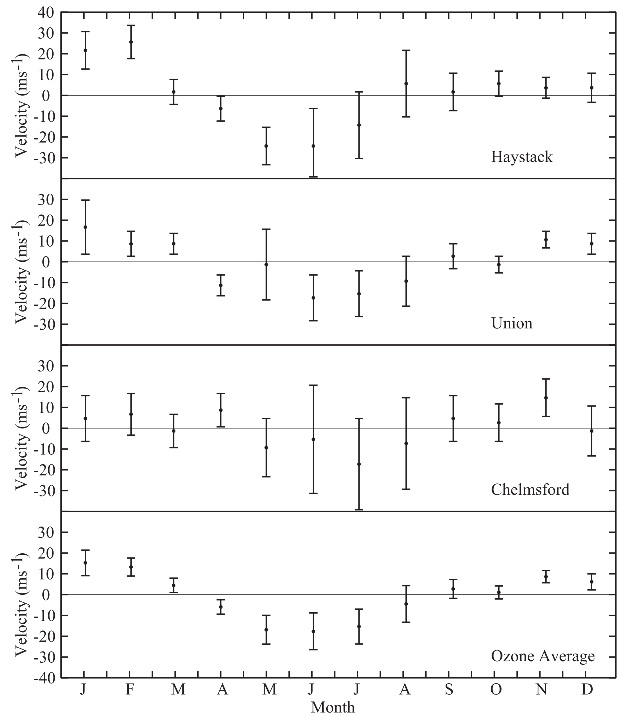

FIG. 1. Seasonal trend in the average velocity of ozone at night. The error bars are $\pm1\sigma$.

2. Instrumentation

The velocity data were acquired from a network of three ozone spectrometers located at the MIT Haystack Observatory (42.618°N, 71.498°W), Union College (42.817°N, 73.928°W), and Chelmsford High School (42.619°N, 71.367°W). The spectrometers are pointed at azimuths 190°, 180°, and 172°, respectively. The beam of each spectrometer physically intersects the ozone layer at 95 km at 38°N, 71°W, which is in the Atlantic Ocean about 200 km off the coast of Maryland. Data at Haystack were taken from 24 January 2009 through 13 August 2014. Data at Union College were taken from 19 February 2009 through 8 June 2015. Finally, data at Chelmsford High School were taken from 25 December 2011 through 8 June 2015. The three spectrometers use temperature-controlled oven crystal oscillators at 10 MHz as a frequency reference. Tests were made of the accuracy of the reference by injecting a test signal at 11.072 454 5 GHz from a synthesizer whose reference had been checked against an atomic clock. The accuracy of the frequency control of the ozone spectrometers was estimated to be within 7 parts in 10^9, corresponding to a line-of-sight velocity accuracy of 2 m s^{-1}. Ozone spectrometers collect wind velocity data during nighttime only (Rogers et al. 2009). Daytime data are not available due to the annihilation of most of the ozone at 95 km by ultraviolet photons from the sun. This reduces the opacity by a factor of about 10 (Smith and Marsh 2005) and reduces the signal to a few millikelvins, resulting in an insufficient signal-to-noise ratio (SNR).

Information on the temperature of the ozone in the mesosphere and lower thermosphere (MLT) can be obtained from the line shape near the peak, where the width is determined primarily from the Doppler broadening of the ozone above about 90 km. However, the results we report in this paper are obtained from single-channel spectrometers for which the SNR is insufficient to obtain measurements of temperature with integration times of less than several weeks. In the future, following the spectrometer enhancements, which will be discussed in section 6, we may be able to obtain temperatures on time scales of geophysical relevance.

3. Results

Figures 1 and 2 show velocity data from the MOSAIC spectrometers at Haystack, Union, and Chelmsford. By convention, negative velocities denote winds directed southward (northerly wind), and positive velocities denote winds directed northward (southerly wind). To

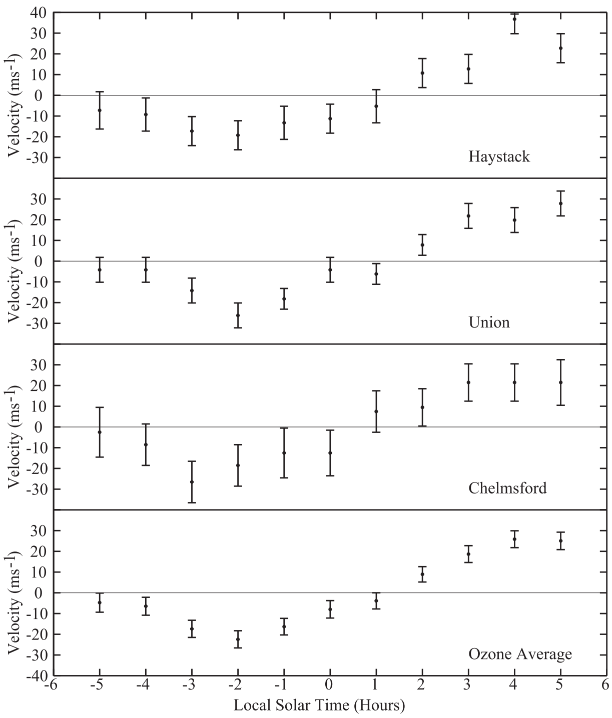

FIG. 2. Trend in the velocity of ozone averaged over all seasons with local time where 0 h corresponds to midnight. The error bars are $\pm 1\sigma$.

reveal the general seasonal variation, data were averaged over nighttime hours for each day of each year. Figure 1 shows the weighted mean for each month. The weighted standard deviation of the errors in each bin was used to plot the error bars on each data point. We note that the meridional winds are northerly in the summer and southerly in the winter. The velocity appears to cross the zero mark twice, roughly around April and September, with northerly winds in between and southerly winds otherwise. The peak-to-peak amplitude in the average is about 30 m s^{-1}, considering a minimum velocity of about -20 m s^{-1} in June–July and a maximum velocity of about $+15$ m s^{-1} in January.

The error bars show significant variation between sites and with season. The larger errors evident in the average of Fig. 1 in the summer and to a lesser extent in the winter are due to lower ozone concentration, which results in lower SNR (Rogers et al. 2009). The variations between sites are the result of different weather conditions, which change system noise. For example, in a period of wet weather, almost all the time with rain will be lost, while periods with rain clouds will typically raise the system noise temperature by a factor of 2. We note that velocity points from the Haystack spectrometer in January and February are higher than those from the other two sites. While this is only marginally statistically significant given the large instrumental noise in the ozone data, it could be related to a longer time coverage by the Haystack spectrometer (2009–15) that includes a period of very low solar activity and potential dependence of MLT winds on solar activity or quasi-biennial oscillation (Forbes et al. 2008; Oberheide et al. 2009). In addition, a frequency error could be responsible. The Haystack spectrometer electronics is the only one of the network's three spectrometers whose data are used in this paper that is located in an unheated building. The new spectrometers will be equipped with a stable frequency reference as will be discussed in section 6.

Figure 2 reveals significant local time variation, in that there are southward winds from -5 through $+1$ h local solar time, and northward winds from $+2$ through $+5$ h. The transition point appears to be within 2 h after midnight, and the full transition is from about -20 to $+25$ m s^{-1} in amplitude. Data for all the available years were binned by month and averaged for each hour. The weighted standard deviation in the errors in each bin was again used to plot the error bars for each data point. The data and local time variation from all three sites are in good agreement. Additionally, the magnitude in the local time variation appears to be larger than the magnitude in the seasonal variation, raising the concern that the observed seasonal behavior may be influenced by a changing phase of diurnal and semidiurnal components of the atmospheric tide. This will be discussed further in section 5.

4. Comparison with Millstone Hill Fábry–Perot data

The Millstone Hill high-resolution Fábry–Perot interferometer (FPI) is located near the MIT Haystack Observatory, specifically at 42.62°N, 71.45°W, where the mean local solar time lags behind universal time (UT) by 4 h and 46 min. The FPI has essentially the same mean local solar time as the region sampled by the ozone spectrometers. The instrument has a 100-mm aperture and is pressure tuned. A standard observation involves four optical measurements at 45° elevation taken at azimuths 0°, 90°, 180°, and 270°, plus a fifth measurement at the zenith. One of the measured parameters is the Doppler shift of the 557.7-nm "green" spectral line nightglow from atomic oxygen, which has peak emission at an altitude of 95 km with a half-width half-intensity of 8 km (Gao et al. 2012; Phillips et al. 1994). This makes the altitude of the green line consistent with the altitude of the ozone line at 95 km.

Because of high optical background illumination from the solar excitation of atomic oxygen (Hedin et al. 2009),

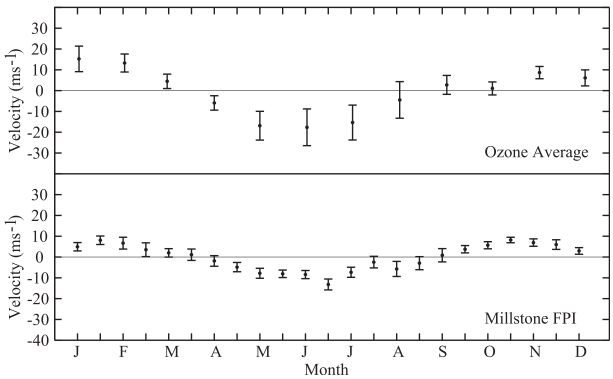

FIG. 3. Comparison of the average meridional velocities of ozone, with error bars $\pm 1\sigma$, and the velocities from the oxygen green line, with error bars $\pm 3\sigma$, by season.

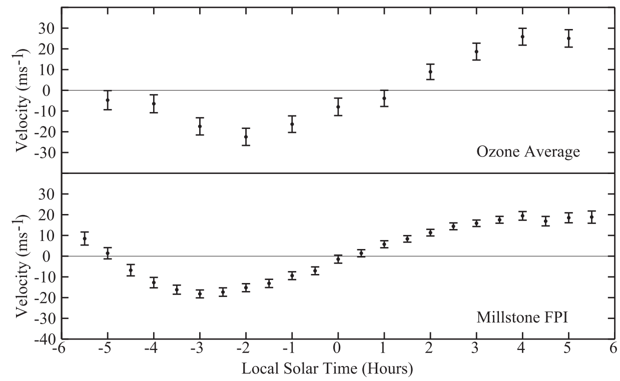

FIG. 4. Comparison of the average meridional velocities of ozone, with error bars $\pm 1\sigma$, and the velocities from the oxygen green line, with error bars $\pm 3\sigma$, by local solar time.

the FPI does not take measurements during daytime hours. Scattering from other atmospheric particles and micrometeors also hampers the ability to acquire precise measurements during the day. Therefore, our analysis of the FPI data from the atomic oxygen nightglow is limited to ±5.5 h local solar time. The FPI wind data consist of 692 nights downloaded from the Coupling, Energetics, and Dynamics of Atmospheric Regions (CEDAR) Archival Madrigal Database[2] and cover the period from 1 December 2012 through 6 October 2015.

Figures 3 and 4 compare the average meridional winds measured by ozone spectrometers and FPI at different seasons and local solar times, respectively. Both seasonal and local time variations obtained from two techniques appear to correlate reasonably well although the ozone results show a larger seasonal variation and a slightly larger local time variation. These differences could be partly due to the difference in latitude sampled by the two techniques. The FPI sampled the MLT at 43°N, while the ozone spectrometers sampled the MLT at 38°N. The FPI winds originate from the north in the summer of the Northern Hemisphere and from the south in the winter. Furthermore, there is a gradual increase from northerly to southerly winds between −4 and +5 h local solar time. The uncertainties given by the FPI data originate from statistical variations in the wind and are not associated with instrumental noise, whereas the uncertainties in the wind velocities from the ozone spectrometers are largely limited by instrumental noise. In particular, since the individual FPI instrumental error values are low (less than $1.0\,\mathrm{m\,s^{-1}}$ on average), the errors are estimated from the root-mean-square (rms) departure from the mean in each bin and 3σ error bars are plotted for the FPI data.

Figure 5 provides a more detailed comparison of the meridional winds measured by the ozone spectrometers and FPI. Both instruments reveal very similar seasonal

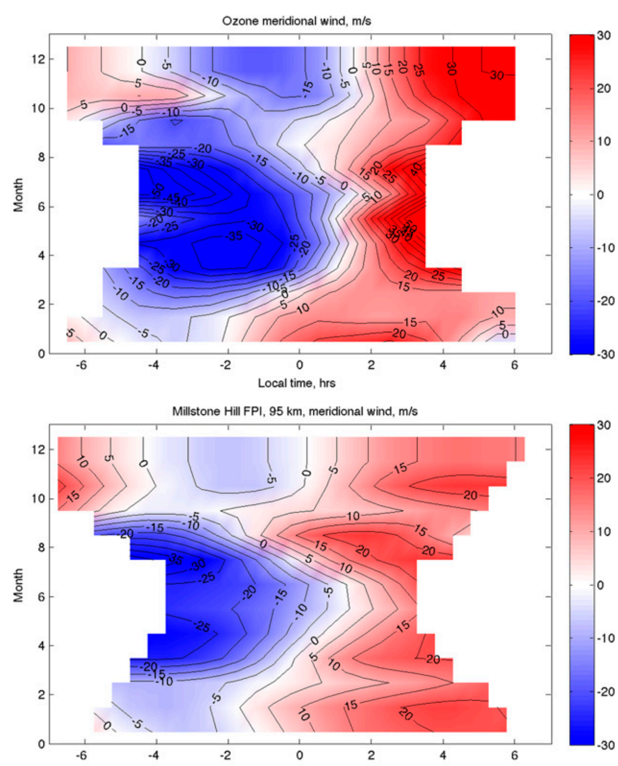

FIG. 5. Meridional winds as a function of season and local time as measured by the (top) ozone spectrometer and (bottom) Millstone FPI.

[2] CEDAR is a U.S. National Science Foundation program for studies of the upper atmosphere. The community database containing Millstone Hill FPI data is located online (at http://madrigal.haystack.mit.edu/).

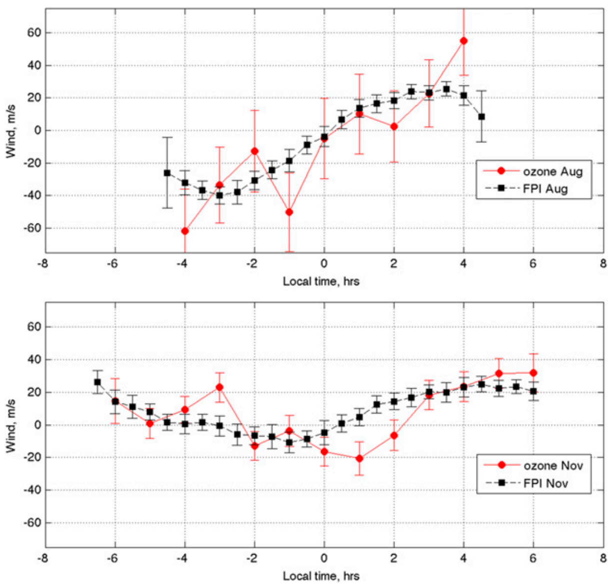

FIG. 6. Comparison of ozone spectrometer and Millstone FPI wind in (top) August and (bottom) November. The error bars for ozone are $\pm 1\sigma$ and $\pm 3\sigma$ for the oxygen green line.

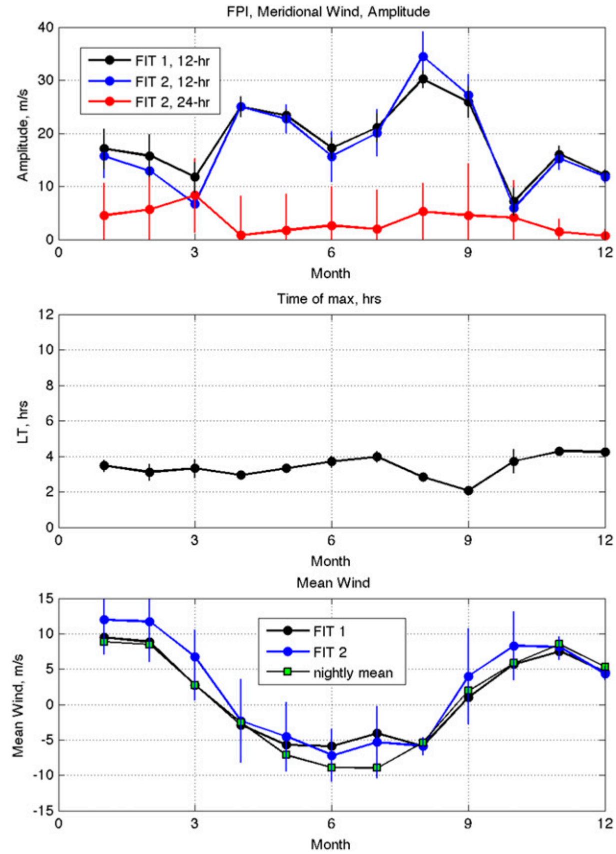

FIG. 7. Seasonal variation in (top) amplitudes, (middle) phase (time of maximum), and (bottom) background meridional wind obtained by Millstone FPI.

structures. In particular, during the equinoxes and summer season, enhancement in the southward wind is observed prior to the local midnight and enhancement in the northward wind is observed after the local midnight, indicating the dominance of tidal characteristics in the measured wind. This behavior weakens in June and is consistent with seasonal change in the zonal wind as observed by the FPI (not shown here). Another seasonal feature is observed in wintertime and includes a weakening of the meridional wind, along with a shift in local time for a transition from northward to southward wind. Figure 6 shows these seasonal features in more detail, illustrating that MOSAIC spectrometer and Millstone Hill FPI observations of mesospheric wind variations agree within error bars. We also note that error bars in August are higher than in November. Variability changes in this manner could arise from a seasonal difference in gravity wave drivers due to the filtering effects of the background zonal wind.

5. Effect of diurnal and semidiurnal tides on mean meridional wind

An important question in the interpretation of the nighttime average of meridional wind is whether the same trend and amplitude would be obtained from data averaged over a full 24-h day. To examine this question we performed fits of monthly averaged FPI data using two approaches. In the first test (FIT 1), data were fit with a mean and semidiurnal tide, while in the second test (FIT 2) data were fit with a mean, diurnal, and semidiurnal tide using several fitting constraints. In the FIT 2 test, amplitudes and phases of components were determined using a three-step procedure. During the first step, data were fit with a mean and semidiurnal tide. During the second step, residuals obtained from the first step were fit with a mean and diurnal tide. The third step used phases of semidiurnal and diurnal tides obtained in steps 1 and 2 as known variables to obtain a new fit with a mean, diurnal, and semidiurnal tide. Figure 7 presents results of these tests and shows tidal amplitudes in the top plot, a tidal phase for the 12-h wind component in the middle plot, and a mean wind determined from the two fitting tests and as a simple nightly average in the bottom plot. The semidiurnal tide amplitude shows a significant seasonal variation, with maximums in April–May and August–September and generally lower tides during the winter season. The diurnal tide amplitude is generally around $\sim 5\,\mathrm{m\,s^{-1}}$ or lower, as expected for a midlatitude location where semidiurnal tides in winds dominate diurnal tides. The time of maximum semidiurnal tide remains generally similar, ~3 LT, for all seasons, with a tendency to later local times in winter. The mean winds determined from the FIT 1 and FIT 2 tests along with the nightly mean method show good agreement, with a gradual transition from ~5–10 $\mathrm{m\,s^{-1}}$ northward wind in wintertime to ~5–10 $\mathrm{m\,s^{-1}}$ southward wind in summertime, in other words, with background wind directed from the summer hemisphere to the winter hemisphere.

All mesospheric wind characteristics reported here are consistent with several other earlier observational studies, including incoherent scatter radar, WIND imaging interferometer (WINDII) satellite, and thermosphere–ionosphere–mesosphere–electrodynamics general circulation model (TIME-GCM) results for this location (Goncharenko and Salah 1998; Zhang et al. 2003). However, the MOSAIC observations provide a more detailed view of seasonal variations. Application of tidal fitting procedures described above for FPI to the MOSAIC meridional wind data shows similar seasonal behavior, albeit with higher 12-h amplitudes and large uncertainties in summer due to the limited data coverage.

6. Enhancements in ozone spectrometers

While the results in this paper were obtained using the original single-channel spectrometers described in Rogers et al. (2009), a six-channel spectrometer was developed in 2014 and a two-channel spectrometer with enhanced performance in each channel is currently under test. These new spectrometers use low-cost TV dongles to replace the custom downconverter and peripheral component interconnect (PCI) bus analog-to-digital converter (ADC) card used in the original design. The two-channel spectrometer, which used both polarizations of the low-noise block feed (LNBF), improves the SNR by a factor of 2 or equivalently achieves the same SNR as the original units in a quarter of the time. In addition the power consumption has been reduced from about 50 W to less than 20 W through the use of an Intel Next Unit of Computing (NUC) computer to replace a full-size PC. Using these improvements, an array of antennas with multichannel spectrometers could provide a sufficient SNR to measure mesospheric winds with much shorter integration time, and it could even provide sufficient SNR to measure winds during the day. To improve the frequency calibration, which may be contributing to the errors in the ozone spectrometer data, future spectrometers will be equipped with a ‘‘chip scale’’ atomic clock or GPS-based frequency reference to bring the long-term stability under 1 part per 10^9.

7. Conclusions

Our ozone spectrometer–based mesospheric wind observations compare favorably with the FPI located nearby. A generally good agreement is observed in seasonal and local time variations of meridional wind observed by two types of instruments. Mean mesospheric meridional wind is consistent with interhemispheric wind circulation theories in the mesosphere, also known as pole-to-pole flow and described in Houghton (2002). Earlier work by Yuan et al. (2008) indicated a summer-to-winter pole-to-pole meridional flow of 17 $\mathrm{m\,s^{-1}}$ at 86 km, which is within the range of magnitudes that we have observed at 95 km. We conclude that simple low-cost ozone spectrometers are capable of providing scientific-quality average wind data on long time scales. Improvements in sensitivity achieved with the deployment of larger networks have a significant future potential for better understanding of the dynamics of the mesosphere. Using a global MOSAIC network, further studies of the meridional and zonal velocities of ozone could reveal more information about the earth’s pole-to-pole circulation as well as the dynamics of airflow between the MLT and other regions of Earth’s atmosphere.

Acknowledgments. This work was supported by the Research Experiences for Undergraduates (REU) summer program funded by U.S. National Science Foundation (NSF) Grant AST-1156504. CEDAR Madrigal database activities are supported by NSF Grant AGS-1242204 to the Massachusetts Institute of Technology. We thank the students and staff of the participating schools and universities for their contributions in the acquisition of the data. We also thank the reviewers for their comments, which helped improve the clarity of the paper.

REFERENCES

Forbes, J. M., X. Zhang, S. Palo, J. Russell, C. J. Mertens, and M. Mlynczak, 2008: Tidal variability in the ionospheric dynamo region. *J. Geophys. Res.*, **113**, A02310, doi:10.1029/2007JA012737.

Gao, H., J.-B. Nee, and J. Xu, 2012: The emission of oxygen green line and density of O atom determined by using ISUAL and SABER measurements. *Ann. Geophys.*, **30**, 695–701, doi:10.5194/angeo-30-695-2012.

Goncharenko, L. P., and J. E. Salah, 1998: Climatology and variability of the semidiurnal tide in the lower thermosphere over Millstone Hill. *J. Geophys. Res.*, **103**, 20 715–20 726, doi:10.1029/98JA01435.

Hedin, J., J. Gumbel, J. Stegman, and G. Witt, 2009: Use of O_2 airglow for calibrating direct atomic oxygen measurements from sounding rockets. *Atmos. Meas. Tech.*, **2**, 801–812, doi:10.5194/amt-2-801-2009.

Houghton, J. T., 2002: *The Physics of Atmospheres*. 3rd ed. Cambridge University Press, 320 pp.

Oberheide, J., J. M. Forbes, K. Hausler, Q. Wu, and S. L. Bruinsma, 2009: Tropospheric tides from 80 to 400 km: Propagation, interannual variability, and solar cycle effects. *J. Geophys. Res.*, **114**, D00I05, doi:10.1029/2009JD012388.

Phillips, A., A. H. Manson, C. E. Meek, and E. J. Llewellyn, 1994: A long-term comparison of middle atmosphere winds measured at Saskatoon (52°N, 106°W) by a medium-frequency radar and a Fabry–Perot interferometer. *J. Geophys. Res.*, **99**, 12 923–12 935, doi:10.1029/94JD00618.

Pickett, H. M., R. L. Poynter, E. A. Cohen, M. L. Delisky, J. C. Pearson, and H. S. P. Müller, 1998: Submillimeter, millimeter, and microwave spectral line catalog. *J. Quant. Spectrosc. Radiat. Transfer*, **60**, 883–890, doi:10.1016/S0022-4073(98)00091-0.

Rogers, A. E. E., M. Lekberg, and P. Pratap, 2009: Seasonal and diurnal variations of ozone near the mesopause from observations of the 11.072-GHz line. *J. Atmos. Oceanic Technol.*, **26**, 2192–2199, doi:10.1175/2009JTECHA1291.1.

——, and Coauthors, 2012: Repeatability of the seasonal variations of ozone near the mesopause from observations for the 11.072-GHz line. *J. Atmos. Oceanic Technol.*, **29**, 1492–1504, doi:10.1175/JTECH-D-11-00193.1.

Smith, A. K., and D. R. Marsh, 2005: Processes that account for the ozone maximum at the mesopause. *J. Geophys. Res.*, **110**, 1984–2012, doi:10.1029/2005JD006298.

Yuan, T., C.-Y. She, D. A. Krueger, F. Sassi, R. Garcia, R. G. Roble, H.-L. Liu, and H. Schmidt, 2008: Climatology of mesopause region temperature, zonal wind, and meridional wind over Fort Collins, Colorado (41°N, 105°W), and comparison with model simulations. *J. Geophys. Res.*, **113**, D03105, doi:10.1029/2007JD008697.

Zhang, S. P., L. P. Goncharenko, J. E. Salah, R. G. Roble, and G. G. Shepherd, 2003: Climatology of neutral winds in the lower thermosphere over Millstone Hill (42.6°N) observed from ground and from space. *J. Geophys. Res.*, **108**, 1051, doi:10.1029/2002JA009512.